http://www.aimspress.com/journal/energy

_Research article_

# Optimistic use of battery energy storage system to mitigate grid disturbances in the hybrid power system

**Virendra Sharma\* and Lata Gidwani**

Department of Electrical Engineering, Rajasthan Technical University, Kota, India

**\*  Correspondence:** Email: vsharmakiran@gmail.com.

**Abstract:** Renewable energy (RE) is being continuously penetrated in to the utility grid and RE penetration level has become comparable to the conventional energy. For balancing of energy generation, solar and wind generators are being integrated to the utility grid at same location to form the hybrid power system. This has been achieved by the use of power electronic converters which are non-linear in nature. Further, variability of solar and wind energy generation also deteriorates quality of power in the hybrid grid. Any disturbance developed in the hybrid grid affects system parameters and power flow due to non-linearity of system and variability of RE generation. This has motivated the academicians and researchers to investigate efficient devices to minimize effects of disturbances on the performance of hybrid grid parameters in the presence of RE. A design of hybrid power system incorporating the wind energy, solar energy, loads, battery energy storage system (BESS) and conventional generator is proposed. This will help to minimize effects of grid disturbances on hybrid power system and improve the performance of utility grid with high RE penetration. Minimization of variability in power generation due to variations of wind speed and solar insolation will be achieved. This is achieved by application of battery energy storage system supported by distribution static compensator (DSTATCOM) controlled by the use of synchronous reference frame theory (SRFT). Test network consisting of five buses, conventional generator, loads, wind generator and solar photovoltaic (PV) generator is realized in MATLAB to establish effectiveness of proposed scheme.

**Keywords:** battery energy storage system; distribution static compensator; hybrid power system; solar energy; synchronous reference frame theory; wind energy

# 1. Introduction

Power system network is continuously becoming complex due to the high penetration level of renewable energy (RE). Further, decentralized generation system concepts are gaining popularity due to the use of distributed generation systems (DGS) using RE. Hence, utility grid is incorporating RE to meet out future demand of energy to form the hybrid power system [1]. Main disadvantage of RE is their non-dispatchable nature. This makes output of RE generation to fluctuate depending on weather conditions such as variations in solar radiation or wind velocities. This results in temporal mismatch of supply and demand. Further, variability of RE generation also deteriorates the voltage profile and variations in the output active and reactive powers. The temporal mismatch, voltage profile and variations in active and reactive power can be managed by the use of battery energy storage system. Grid disturbances in the hybrid power system network due to high penetration of both wind energy and solar energy become prominent in the utility grid. These can be mitigated by the use of energy storage devices to balance the intermittency. It stores the excess PV power available when load demand reduces on the grid. On the other hand, it discharges when the demand rises or when RE generation reduces [2]. Significant research work is reported on the hybrid applications of wind energy, solar PV energy, fuel cell and battery for standalone applications. A very small research work is reported in literature on the grid level use of energy storage devices in coordination with the wind and solar PV energy to mitigate the effects of grid disturbances. Chee et al. [3], proposed a real-time energy management system (EMS) for renewable energy using battery energy storage (BESS). The EMS is incorporated to a smart grid to control the power output of the RE/battery system in response to mitigate disturbances of electricity networks. Amit et al. [4], presented an overview of various energy storage systems such as pumped hydro energy storage, compressed air energy storage, battery energy storage, flywheel, super-capacitors, hydrogen energy storage, superconducting magnetic energy storage and thermal energy storage which are used for the mitigation of impacts of grid disturbances with renewable energy sources. Choton et al. [5], provided few recommendations pertaining to procedures, adequate energy storage system (ESS) selection, smart charging and discharging of ESS, sizing of ESS, placement of ESS and operation of ESS, and power quality issues. Hannana et al. [6], presented a detailed study related to power electronics contribution to RE conversion which is implemented for reduction of emission addressing applications, issues, and recommendations. Zhang et al. [7], contributed an optimized design of a hybrid desalination plant of reverse osmosis (RO) consuming the power generated by solar PV and wind energy. Three hybrid propositions such as solar-wind-battery-RO, solar-battery-RO, and wind-battery-RO desalination plants which work automatically had been investigated. Zhang et al. [8], proposed a hybrid algorithm to design optimal size of the stand-alone hybrid system incorporating the wind and solar energy. It is based on the use of chaotic search, harmony search and simulated annealing algorithms. To improve the accuracy of the algorithm weather forecasting for solar radiation, ambient temperature, and wind speed forecasting is achieved using artificial neural networks (ANN). Zhang et al. [9], proposed load forecasting algorithm and an effective method using Tabu Search for optimization of small independent hybrid power schemes (IHPS) incorporating the solar energy, wind and a battery energy storage system. Optimal meet out of load demand and minimized IHPS life cycle cost is achieved. Maleki et al. [10], designed an optimal hybrid energy system using biodiesel fuels, solar PV, battery storage system and a diesel generator. This is used to meet out the backup energy demand of a typical Iranian village household.

Norouzak seed oil is used as a source of biodiesel. It is established that Norouzak fuel is a good candidate for an alternative fuel-hybrid system to meet out the electrical demands of needs of a rural houses with reduced operating cost, increased efficiency and minimum emission of pollutants. A method using evolutionary programming for evaluation of effects of a grid integrated fuel cell based Combined heat and power (CHP) systems is proposed in [11]. Minimum operational cost for application in the residential power supply with minimum constraints is achieved and it is established that hybrid system will be effective to meet out future energy demand. Mahela et al. [12], presented a method using distribution static compensator (DSTATCOM) with BESS for improvement of power quality in the utility grid with wind energy penetration. Load compensation, elimination of harmonics currents, mitigation of voltage flicker, voltage and frequency regulation have been achieved using synchronous reference frame theory (SRFT) based control of DSTATCOM by providing fast control of active and reactive powers. Maleki [13], modelled a grid independent hybrid RE system (GIHRES) using solar PV, wind energy, battery storage, hydrogen, reverse osmosis desalination (ROD) to meet the load demand for increasing the fresh water availability. Sharma et al. [14], designed a Fuzzy logic controller for optimized sizing and location of distributed generation (DG) to improve voltage profile and reduction in active and reactive power losses in real time power network of Rajasthan, India.

Hybrid power systems using the solar PV, wind energy and fuel cell have been reported in literature to meet out the energy demand for backup use and small scale applications. Further, DSTATCOM with BESS has find applications on small scale such as isolated wind energy plant, residential supply arrangement, load compensation and standalone solar PV system. However, very less number of publications had been reported for proposing grid level implementation of battery energy storage system. Hence, there is a need to investigate the methods which may be implemented at grid level to mitigate the disturbances introduced due to high penetration of variable nature wind energy and solar energy into the utility grid. This can be achieved by the use of custom power devices. This has been taken as key feature for investigation.

This research work presents a method for mitigation of impacts of grid disturbances on the performance of utility network in the hybrid power system network incorporated with both wind energy and solar energy penetration. This is achieved by the use of battery energy storage system controlled by DSTATCOM.

This paper is organized in five sections. Starting with introduction in Section 1, Section 2 details the test system and proposed battery energy storage system. Simulation results and their discussion are provided in Section 3. Performance comparison in terms of total harmonic distortion (THD) of voltage and current with and without the proposed BESS is provided in Section 4. Concluding remark is provided in Section 5.

## 2. Test system

Test system of hybrid power system (HPS) interfaced with battery energy storage system (BESS) controlled by the distribution static compensator (DSTATCOM) used for study related to mitigation of Grid Disturbances in Hybrid Power System is detailed in this section. Details of wind energy conversion system (WECS), solar photovoltaic (PV) system and BESS supported by DSTATCOM used in the proposed study are also detailed in this section.

## 2.1. Test network

Test network of HPS integrated to Utility grid and interfaced with doubly fed induction generator (DFIG) based wind energy generation system, solar PV system and BESS is described in Figure 1. Generator G1 used to represent utility grid is integrated to bus B2 through a generator transformer (XFM). Transmission lines of the test network are represented by TRL1, TRL2 and TRL3. Transmission line parameters are detailed in Table 1. All loads have values equal to 2 MW. Details of transformers used in the test network are provided in Table 2. Block diagram showing the AC bus, DC bus and integration of all the sources and loads is shown in Figure 2. In Indian power system network, a local network is developed for the RE plants to which small capacity plants are connected at different locations to collect the power. This test system is integrated to the utility grid. Hence, this system has been considered to simulate the real network used in India for grid integration of RE power plants and can be used to simulate large area networks.
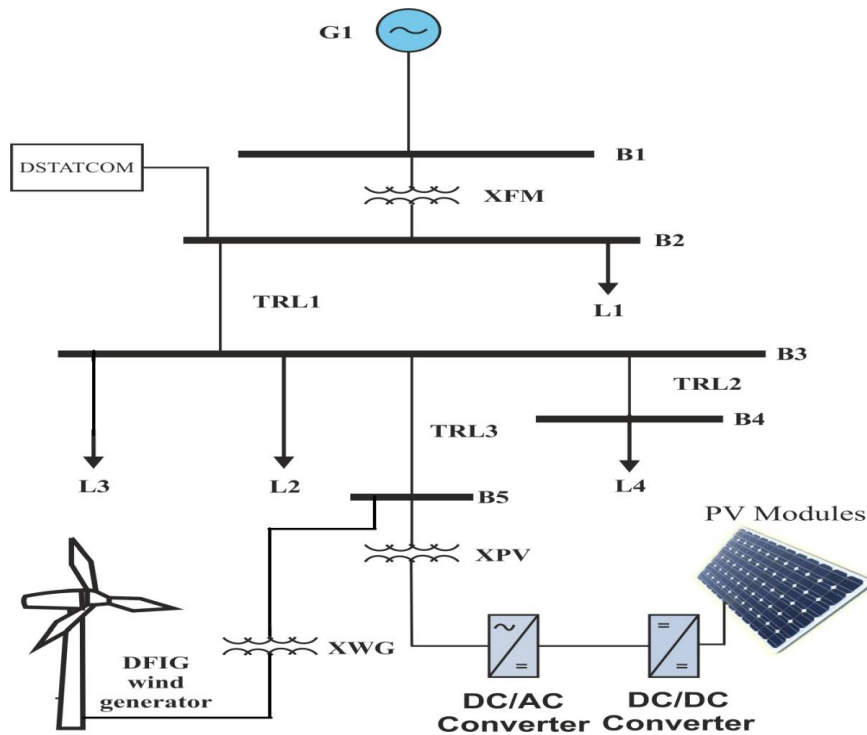


**Figure 1.** Hybrid power test system incorporated with BESS.

**Table 1.** Transmission line parameters of test system.

| S. No. | Transmission Line Parameters | values |
|---|---|---|
| 1 | Positive sequence impedance | $0.1153 + j0.3958 \ \Omega/km$ |
| 2 | Zero sequence impedance | $0.4130 + j1.2516 \ \Omega/km$ |
| 3 | Length of transmission line TRL1 | 14 km |
| 4 | Length of transmission line TRL2 | 14 km |
| 5 | Length of transmission line TRL3 | 2.5 km |

**Table 2.** Transformer parameters of test system.

| Transformer symbol | MVA Rating | Voltage HV winding (kV) | Voltage LV winding (kV) |
|:---:|:---:|:---:|:---:|
| XFM | 47 | 120 | 4.16 |
| XPV | 1 | 4.16 | 0.260 |
| XWG | 3 | 4.16 | 0.575 |
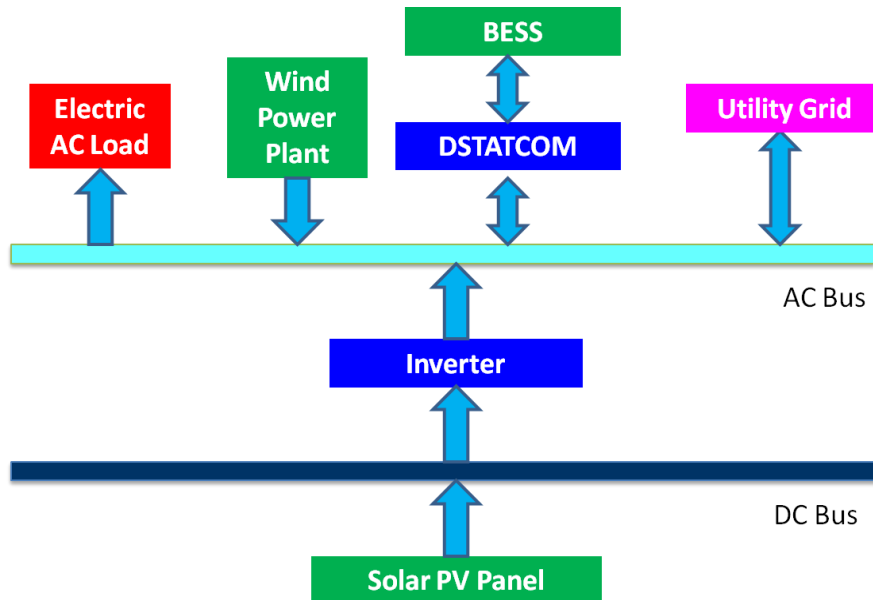


**Figure 2.** Block diagram of hybrid power system.

*2.2. Wind energy conversion system*

Wind energy conversion system (WECS) used for the proposed study is consists of the components such as wind turbine (WT), rotor side converter (RSC), grid side converter (GSC), a doubly fed induction generator (DFIG) and a dc link capacitor. Wind turbine is used to convert kinetic energy of wind speed into mechanical energy of shaft. This mechanical energy is converted to electrical energy using DFIG. WECS used in the study has a rating of 1.5 MW and 60 Hz frequency. The power is delivered at voltage level of 575 V. WECS is integrated to utility grid through transformer XWG at bus B5. The wind speed equal to 11 m/s is used in this study. Parameters reported in [15] are considered for modeling of WECS.

*2.3. Solar PV system*

The solar PV system rated at 100 kW is integrated to test network on bus B5 using a transformer designated as XPV. Technical parameters of the solar PV system as reported in [16] are used in the proposed study. Output direct current (dc) voltage of solar PV system is 273.5 V which is stepped up to 500 V dc using a dc-dc boost converter. A dc to ac inverter is used to convert 500 V dc into 260 V three phase ac Supply. This is stepped up to 4.16 kV using transformer XPV.

## 2.4. Proposed battery energy storage system

Battery energy storage system is integrated on bus B2 of hybrid test power system using three-leg topology of three-phase three-wire DSTATCOM. BESS is connected in parallel with the DC capacitor of DSTATCOM as shown in Figure 3. Active and reactive powers can be exchanged between the DSTATCOM supported BESS and HPS network by varying voltage magnitude of the inverter and phase angle difference between bus voltage and the inverter output [17]. Active and reactive powers exchange can be given by following relations:

$$P = \frac{V_{pcc}V_c \sin(\alpha)}{X} \tag{1}$$

$$Q = \frac{V_{pcc}(V_{pcc} - V_c \cos(\alpha))}{X} \tag{2}$$

where $V_c$ is the inverter voltage; P is the active power exchange; Q is the reactive power exchange; Vpcc is the voltage at point of common coupling (PCC); $\alpha$ is the angle of Vpcc with respect to Vc; X is the reactance of the coupling inductor. Design value of the dc link capacitor used in this study is 10,000 µF which is calculated using the relations reported in [18]. Design value of ac inductor is selected as 40 mH using the relations reported in [19]. Resistance and capacitance of the ripple filter are taken as 0.1 Ω and 10 µF respectively based on the constraints reported in [20]. Voltage of the battery energy storage system is kept at 7000 V and calculated using the relations reported in [21]. Synchronous reference frame theory (SRFT) based control of the DSTATCOM is proposed to achieve exchange of active power and reactive power between the DC link interfaced by BESS and PCC. Proposed BESS supported by DSTATCOM will be effective for all the test system irrespective of the number of buses, number of generators and load. However, compensation provided will depend on the capacity of BESS relative to the total power handled by the test network. Power exchange between PCC and BESS will depend on the rating of BESS.
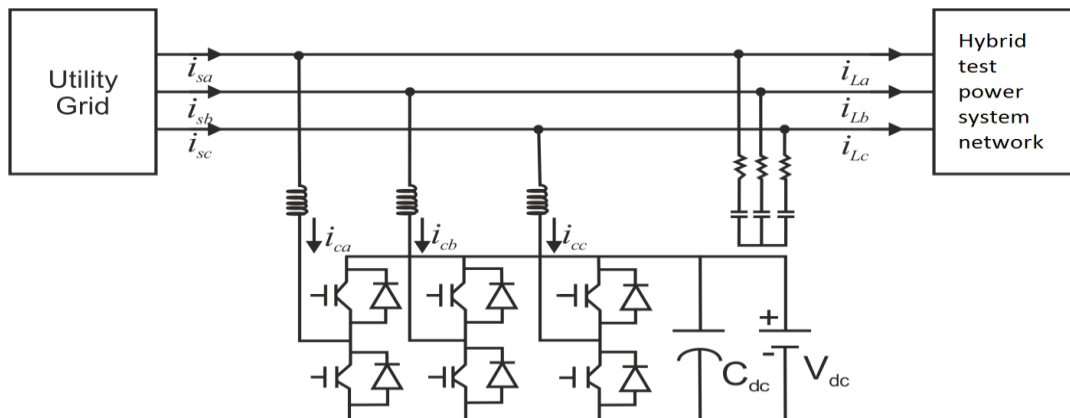


**Figure 3.** Battery energy storage system integrated to hybrid power system using DSTATCOM.

## 3.   Simulation results and discussion

The simulation results related to various case studies with and without BESS to show the

effectiveness of proposed DSTATCOM supported BESS to mitigate disturbances in the utility grid are detailed in this section. Results are plotted for a period of 1 second. Dynamics introduced in all the considered events are observed only for duration of 0.05 s. Hence, a period of 1 s is sufficient to capture the dynamics introduced in the voltage waveforms, plots of active and reactive powers. Discussion of simulation results is also presented in this section.

*3.1. Switching on the resistive load*

Simulation results and their discussion during the event of switching on the resistive load in the absence as well as presence of BESS supported by DSTATCOM are provided in following subsections.

3.1.1.  Absence of BESS

A resistive load rated at 2 MW is switched on at 0.5 s in the absence of BESS. Voltage signal is recorded at PCC and depicted in Figure 4. It is observed that voltage suddenly dips by 5 V and final settle at a value lower by 2 V. Hence, decrease in voltage is observed by switching ON the resistive load along with a disturbance.
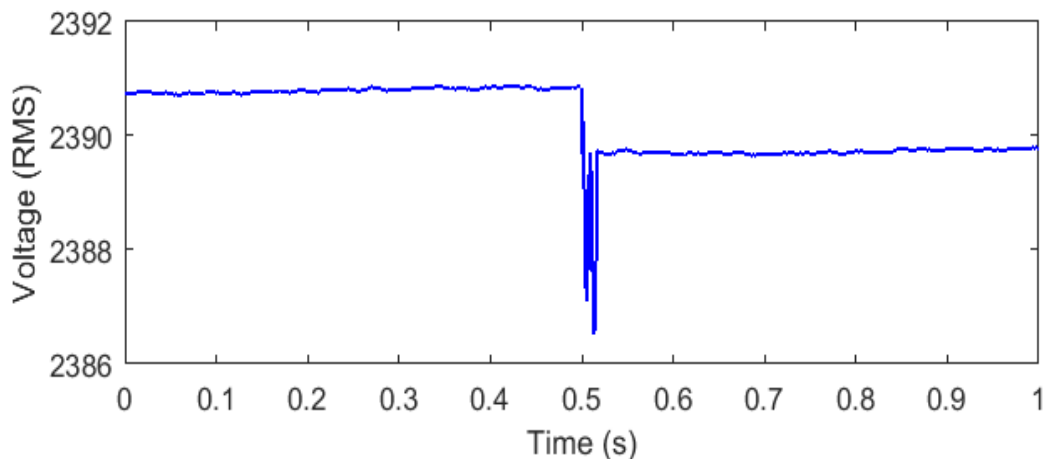


**Figure 4.** Voltage at PCC during the event of switching on the resistive load in the absence of BESS.

A resistive load rated at 2 MW is switched on at 0.5 s in the absence of BESS. Active power supplied by the source, consumed by the load and supplied by the BESS supported by DSTATCOM is shown in Figure 5(a). Reactive power supplied by the source, consumed by the load and supplied by the BESS supported by DSTATCOM is shown in Figure 5(b).
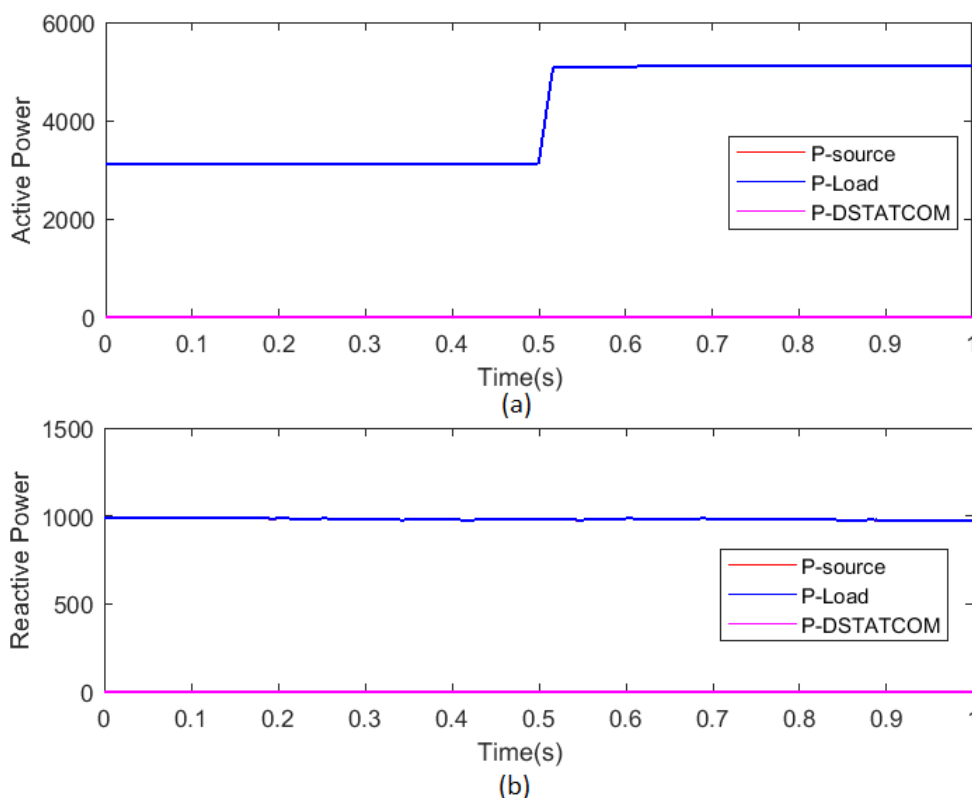
**Figure 5.** Power flow during the event of switching on the resistive load in the absence of BESS (a) active power flow (b) reactive power flow.

This can be observed from the Figure 5(a) that power supplied by the BESS is zero before and after the event because the BESS is kept out of the circuit. The active power supplied by the source is consumed by the load. Hence, curve of active power consumed by load superimposes the active power supplied by the source. Further, the active power supplied by the source increases after the event of switching ON the resistive load due to increased value of the load. It is also observed from the Figure 5(b) that reactive power supplied by the BESS supported by DSTATCOM is zero because the BESS is kept out of circuit. Further, there is no change in the values of reactive power consumed by the test network because reactive power is not consumed by the resistive load. The reactive power consumed by the test network follows the curve of reactive power supplied by the source.

### 3.1.2.    Presence of BESS

A resistive load rated at 2 MW is switched on at 0.5 s in the presence of BESS. Voltage signal is recorded at PCC and depicted in Figure 6. It is observed that voltage suddenly dips by 3 V indicating that change in voltage level has been reduced the use of the BESS supported by DSTATCOM. Hence, voltage profile improves by 40%. Further, the magnitude of the voltage after the event of switching on the resistive load is all most equal to the voltage magnitude before the event. Hence, voltage has been improved and disturbance level has been decreased in the utility network by the use of BESS supported by DSTATCOM.
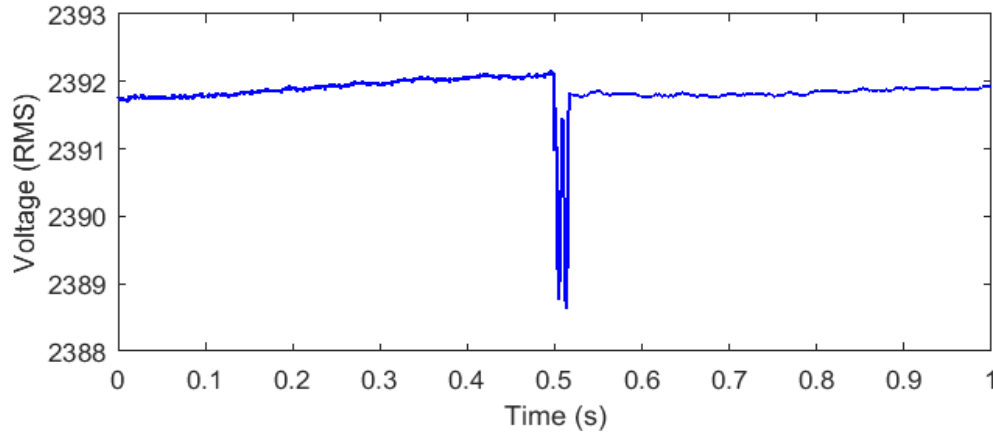
**Figure 6.** Voltage at PCC during the event of switching on the resistive load with BESS.

A resistive load rated at 2 MW is switched on at 0.5 s in the presence of BESS. Active power supplied by the source, consumed by the load and supplied by the BESS supported by DSTATCOM is shown in Figure 7(a). Reactive power supplied by the source, consumed by the load and supplied by the BESS supported by DSTATCOM is shown in Figure 7(b).
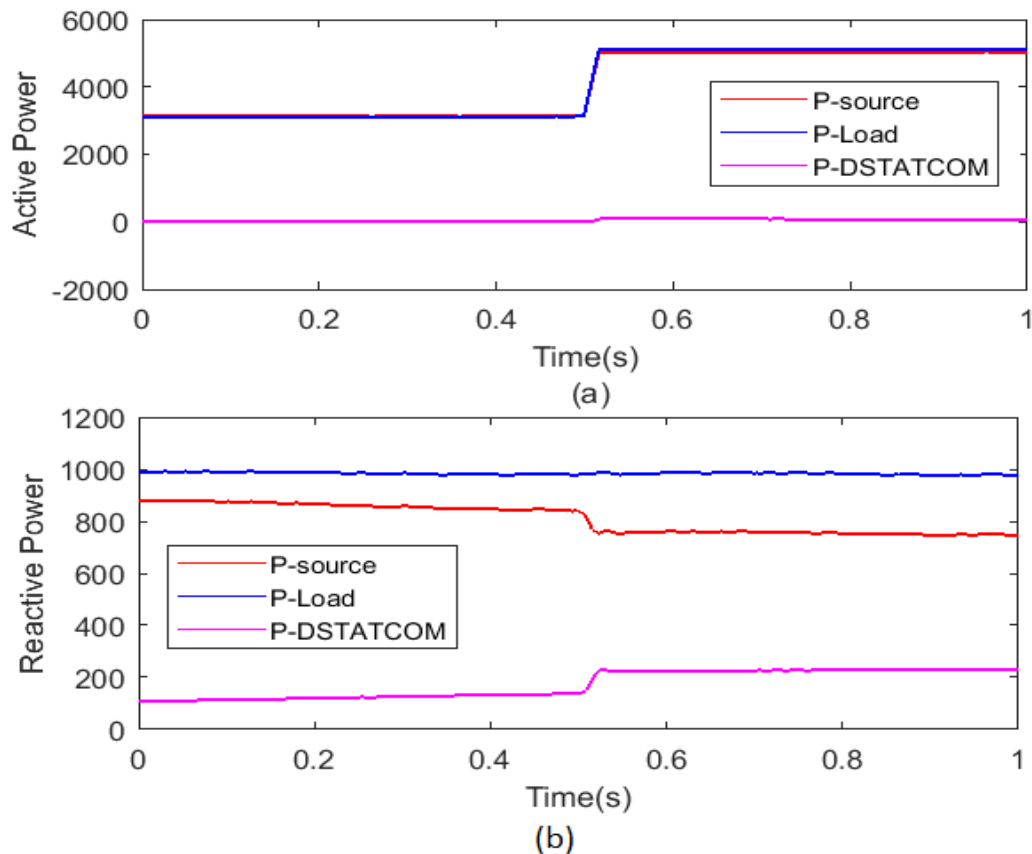


**Figure 7.** Power flow during the event of switching on the resistive load in the presence of BESS (a) active power flow (b) reactive power flow.

This can be observed from the Figure 7(a) that power supplied by the BESS is zero before the event because power demanded by load is supplied by the source. However, after the event, the BESS supplies the power (100 kW) to meet out increased demand. Hence, curve of the active power demanded by the load superimposes before the event and after the event the sum of source power and power supplied by the BESS supported by DSTATCOM is equal to the power drawn by the test network. It is also observed by the Figure 7(b) that reactive power supplied by the BESS supported by DSTATCOM is non-zero (100 kV Ar) because the dc link capacitor of the DSTATCOM supplies the reactive power to the test network. Reactive power supplied by the DSTATCOM also increases after the event to regulate the voltage.

### 3.2. Switching off the resistive load

Simulation results and their discussion during the event of switching off the resistive load in the absence as well as presence of BESS supported by DSTATCOM are provided in following subsections.

### 3.2.1. Absence of BESS

A resistive load rated at 2 MW connected on bus B2 of test system is switched off at 0.5 s in the absence of BESS. Voltage signal is recorded at PCC and depicted in Figure 8. It is observed that a high magnitude transient is observed at the time of switching off the resistive load in the absence of BESS. The voltage magnitude is same before and after the event.
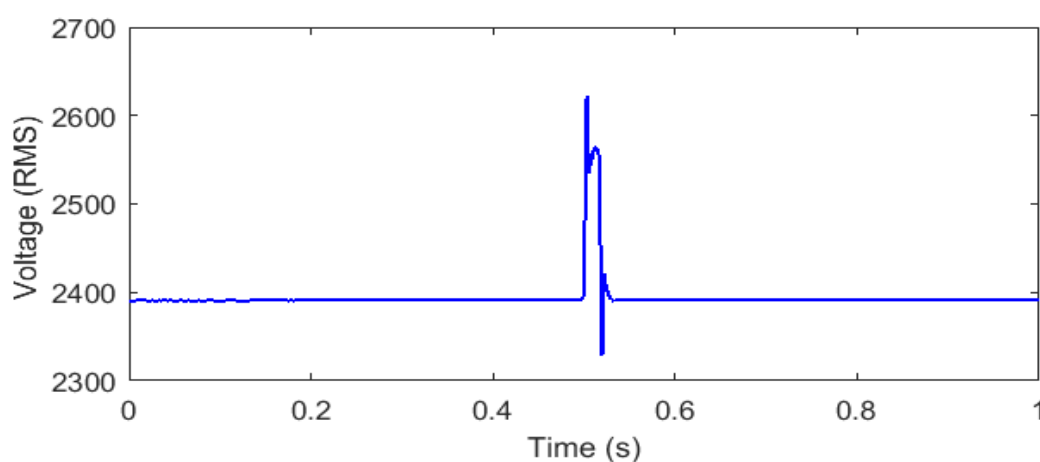


**Figure 8.** Voltage at PCC during the event of switching off the resistive load without BESS.

A resistive load rated at 2 MW connected on bus B2 of test system is switched off at 0.5 s in the absence of BESS. Active power supplied by the source, consumed by the load and supplied by the BESS supported by DSTATCOM is shown in Figure 9(a). Reactive power supplied by the source, consumed by the load and supplied by the BESS supported by DSTATCOM during the event of switching off the load in the absence of BESS is shown in Figure 9(b).

This can be observed from the Figure 9(a) that power supplied by the BESS is zero before and

after the event because the BESS is kept out of the circuit. The active power supplied by the source is consumed by the load. Hence, curve of active power consumed by load superimposes the active power supplied by the source. Further, the active power supplied by the source decrease after the event of switching off the resistive load due to decreased value of the load. It is also observed by the Figure 9(b) that reactive power supplied by the BESS supported by DSTATCOM is zero because the BESS is kept out of circuit. Further, there is no change in the values of reactive power consumed by the test network before and after the event because reactive power is not consumed by the resistive load. However, reactive power consumed by the test network is increased at the time of event for short duration of 0.04 s and used to mitigate the voltage disturbance. The reactive power consumed by the test network follows the curve of reactive power supplied by the source.
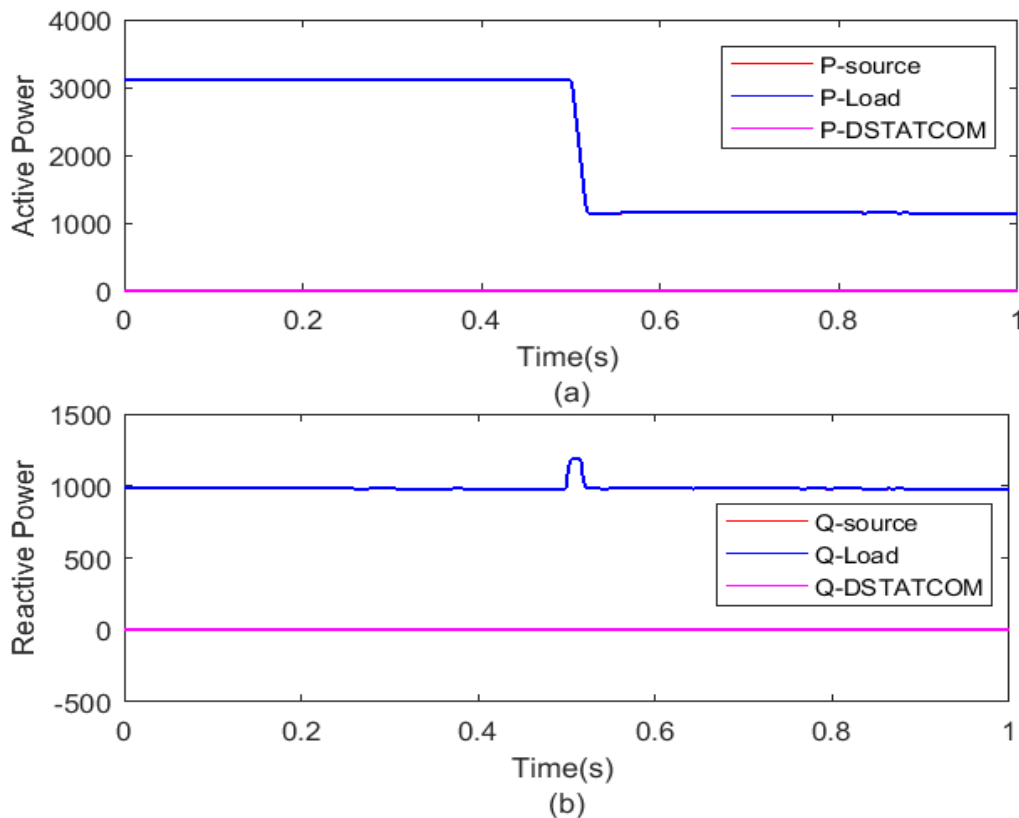


**Figure 9.** Power flow during the event of switching off the resistive load in the absence of BESS (a) active power flow (b) reactive power flow.

### 3.2.2. Presence of BESS

A resistive load rated at 2 MW connected on bus B2 of test system is switched off at 0.5 s in the presence of BESS. Voltage signal is recorded at PCC and depicted in Figure 10. It is observed that a transient of high magnitude is detected at the time of switching off the resistive load in the presence of BESS. However, the magnitude of transient voltage has been reduced by small values (10%) due to the use of BESS supported by DSTATCOM. The voltage magnitude is same before and after the event.
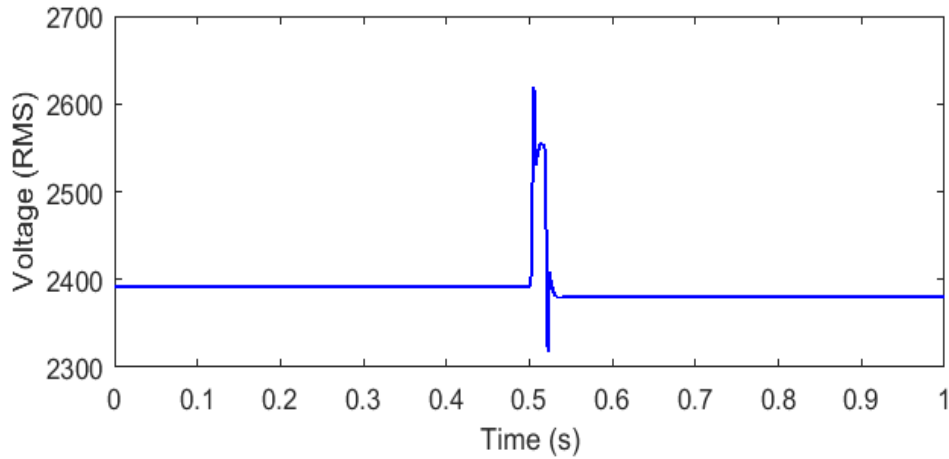
**Figure 10.** Voltage at PCC during the event of switching off the resistive load in the presence of BESS.
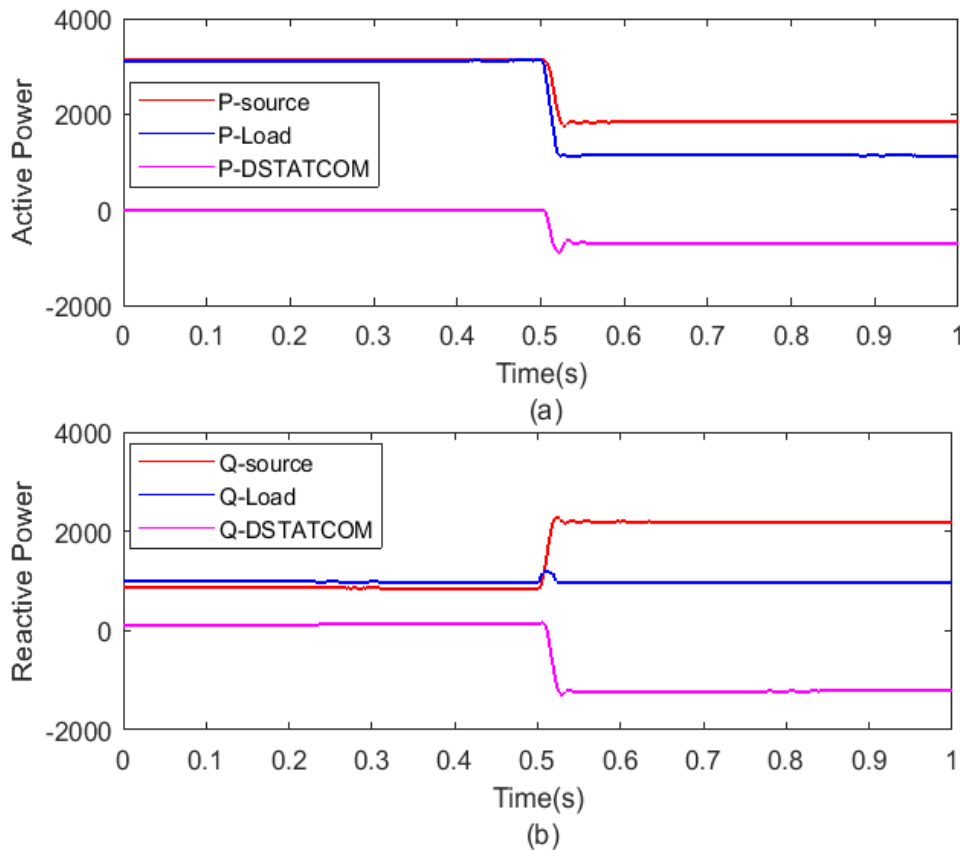


**Figure 11.** Power flow during the event of switching off the resistive load in the presence of BESS (a) active power flow (b) reactive power flow.

A resistive load rated at 2 MW connected on bus B2 of test system is switched off at 0.5 s in the presence of BESS. Active power supplied by the source, consumed by the load and supplied by the BESS supported by DSTATCOM is shown in Figure 11(a). Reactive power supplied by the source,

consumed by the load and supplied by the BESS supported by DSTATCOM during the event of switching off the load in the presence of BESS is shown in Figure 11(b).

This can be observed from the Figure 11(a) that power supplied by the BESS is zero before the event and active power supplied by the source is consumed by the load. Hence, curve of active power consumed by load superimposes the active power supplied by the source before the event. Further, the active power supplied by the source decrease after the event of switching off the resistive load due to decreased value of the load and BESS starts storing the active power due to decreased demand. Sum of active power taken by test network and power supplied by BESS will be equal to the power supplied by source. It is also observed by the Figure 11(b) that reactive power supplied by the BESS supported by DSTATCOM is zero before the event and after the event dc link capacitor starts absorbing the reactive power which will be supplied by the source. Further, there is no change in the values of reactive power consumed by the test network because reactive power is not consumed by the resistive load. However, reactive power consumed by the test network is increased at the time of event and used to mitigate the voltage disturbance.

### 3.3. Outage of wind generator

Simulation results and their discussion during the event of outage of wind generator in the absence as well as presence of BESS supported by DSTATCOM are provided in following subsections.

### 3.3.1.    Absence of BESS

Wind generator rated at 1.5 MW and already connected on bus B5 of test system is switched off at 0.5 s in the absence of BESS. Voltage signal is recorded at PCC and depicted in Figure 12. It is observed that voltage decreases after the event of outage of wind generator by 6 V in the absence of BESS. A transient voltage of low magnitude is also observed at the time of outage of wind generator.
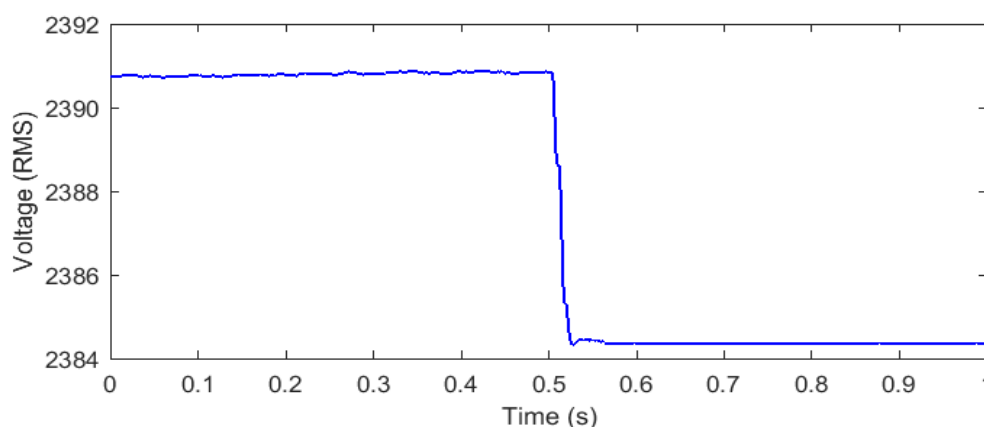


**Figure 12**. Voltage at PCC during the event of outage of wind generator without BESS.

The wind generator of capacity 1.5 MW already connected on bus B5 of test system is switched off at 0.5 s in the absence of BESS. Active power supplied by the source, consumed by the load and

supplied by the BESS supported by DSTATCOM is shown in Figure 13(a). Reactive power supplied by the source, consumed by the load and supplied by the BESS supported by DSTATCOM during the event of outage of wind generator in the absence of BESS is shown in Figure 13(b).
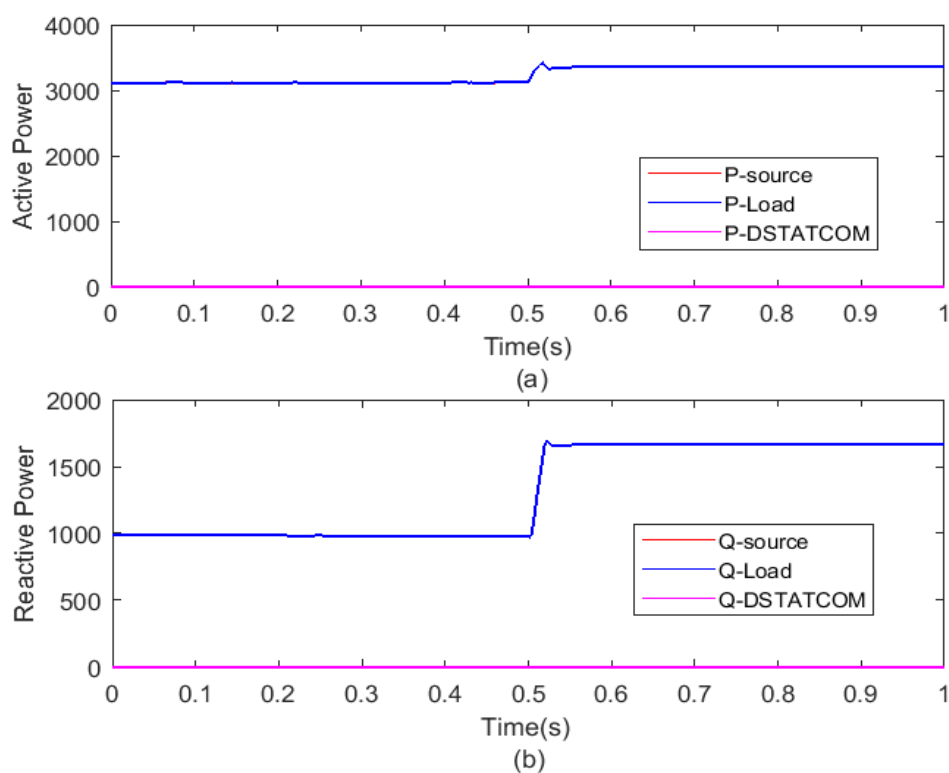


**Figure 13.** Power flow during the event of outage of wind generator without BESS (a) active power flow (b) reactive power flow.

This can be observed from the Figure 13(a) that power supplied by the BESS is zero before and after the outage of wind generator because the BESS is kept out of the circuit. The active power supplied by the source is consumed by the load. Hence, curve of active power consumed by load superimposes over the active power supplied by the source. Further, the active power supplied by the source increases after the event of outage of wind generator due to reduction in the local generation available in the test network. It is also observed by the Figure 13(b) that reactive power supplied by the BESS supported by DSTATCOM is zero because the BESS is kept out of circuit. Further, reactive power consumed by the test network has been increased due to reduction in reactive power supplied by the capacitors installed in the wind power plant. Increased reactive power demand is supplied by the source. The reactive power consumed by the test network follows the curve of reactive power supplied by the source. A transient component of reactive power is also observed at the time of outage of wind generator.

### 3.3.2. Presence of BESS

The wind generator of capacity 1.5 MW already connected on bus B5 of test system is switched off at 0.5 s in the presence of BESS. Voltage signal is recorded at PCC and depicted in Figure 14. It

is observed that voltage decreases by small magnitude (15%) after the event of outage of wind generator by 6 V in the presence of BESS. Transient voltage is not observed at the time of outage of wind generator in the presence of BESS.
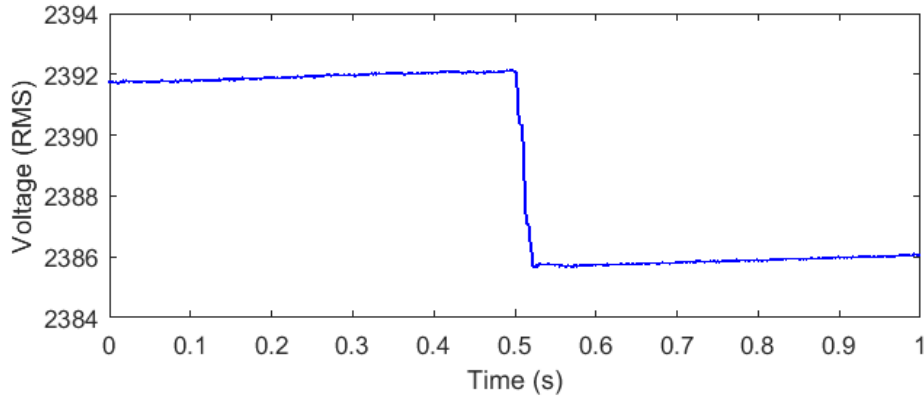


**Figure 14.** Voltage at PCC during the event of outage of wind generator with BESS.
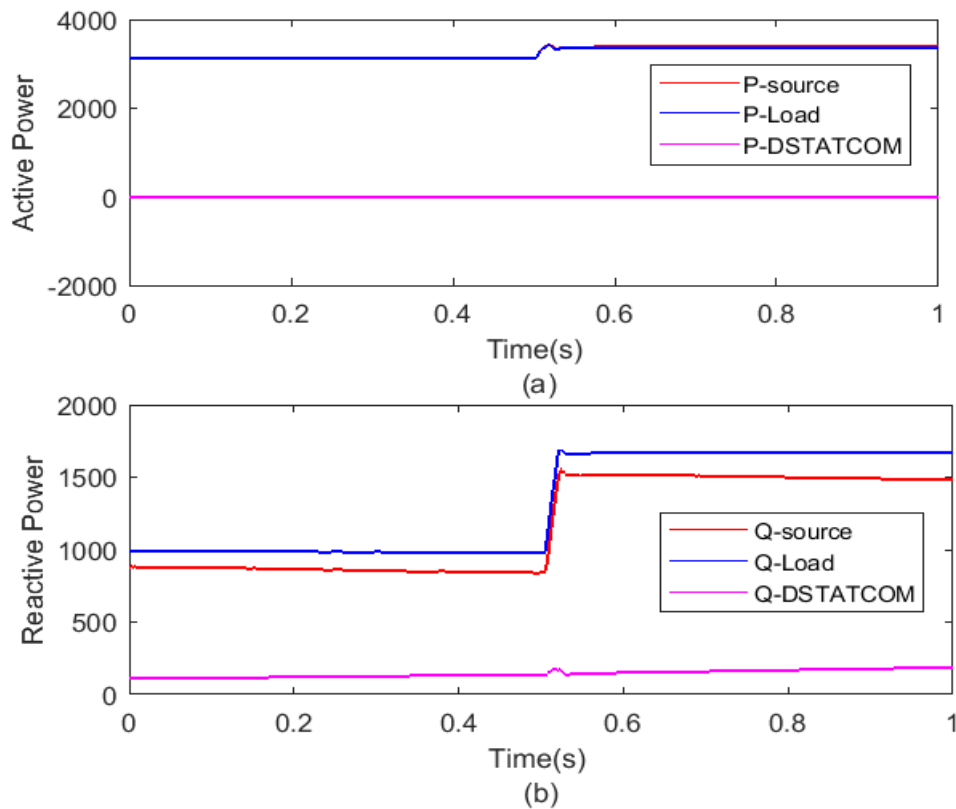


**Figure 15.** Power flow during the event of outage of wind generator with BESS (a) active power flow (b) reactive power flow.

The wind generator of capacity 1.5 MW already connected on bus B5 of test system is switched off at 0.5 s in the presence of BESS. Active power supplied by the source, consumed by the load and

supplied by the BESS supported by DSTATCOM is shown in Figure 15(a). Reactive power supplied by the source, consumed by the load and supplied by the BESS supported by DSTATCOM during the event of outage of wind generator in the presence of BESS is shown in Figure 15(b).

This can be observed from the Figure 15(a) that power supplied by the BESS is nearly zero before outage of wind generator. However, after outage event there is small exchange of power with the BESS. Therefore, active power supplied by the source is consumed by the load. Hence, curve of active power consumed by load superimposes over the active power supplied by the source. Further, the active power supplied by the source increases after the event of outage of wind generator due to reduction in the local generation available in the test network. Transient power component at the time of outage of wind generator has been reduced significantly. It is also observed from the Figure 15(b) that BESS supported by DSTATCOM continuously supplies reactive power before and after the event of outage of wind generator in the presence of BESS. Transient component of reactive power observed at the time of outage of wind generator has been reduced significantly by the use of BESS supported by DSTATCOM.

### 3.4. Simultaneous outage of both wind and solar PV generators

Simulation results and their discussion during the event of simultaneous outage of wind plant and solar PV plant in the absence as well as presence of BESS supported by DSTATCOM are provided in following subsections.

#### 3.4.1. Absence of BESS

The simultaneous outage of wind and solar PV generators integrated on bus B5 of test system is performed at 0.5 s in the absence of BESS. Voltage signal is recorded at PCC and depicted in Figure 16. It is observed that due to the event of simultaneous outage of both wind and solar PV generators, the voltage decreases by an amount of 10 V. A transient voltage with sharp dip is also observed at the time of simultaneous outage of both wind and solar PV generators.
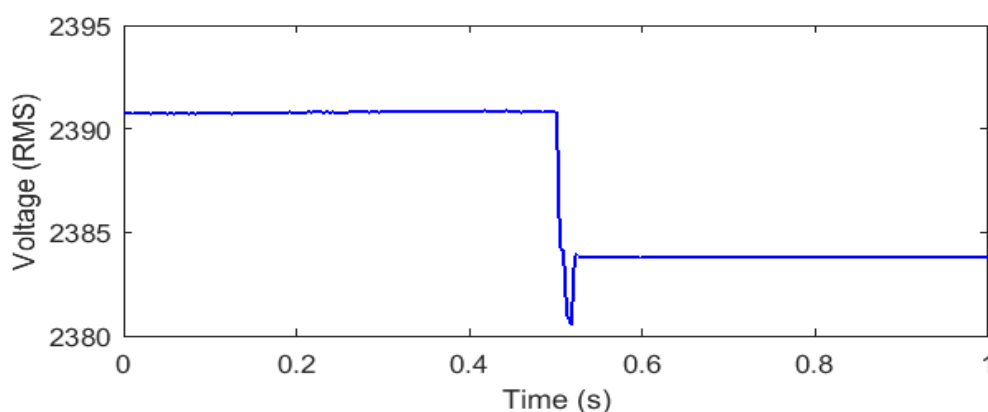


**Figure 16.** Voltage at PCC during the event of simultaneous outage of both wind and solar PV generators without BESS.

The simultaneous outage of wind and solar PV generators integrated on bus B5 of test system is performed at 0.5 s in the absence of BESS. Active power supplied by the source, consumed by the load and supplied by the BESS supported by DSTATCOM is shown in Figure 17(a). Reactive power supplied by the source, consumed by the load and supplied by the BESS supported by DSTATCOM during the event of simultaneous outage of wind and solar PV generators in the absence of BESS is shown in Figure 17(b).

This can be observed from the Figure 17(a) that power supplied by the BESS is zero before and after the simultaneous outage of wind and solar PV generators because the BESS is kept out of the circuit. The active power supplied by the source is consumed by the load. Hence, curve of active power consumed by load superimposes over the active power supplied by the source. Further, the active power supplied by the source increases after the event of simultaneous outage of wind and solar PV generators due to reduction in the local generation available in the test network. A low magnitude power transient is also observed at the time of simultaneous outage of wind and solar PV generators. It is also observed by the Figure 17(b) that reactive power supplied by the BESS supported by DSTATCOM is zero because the BESS is kept out of circuit. Further, reactive power drawn by the test network from the source has been increased due to reduction in the reactive power supplied by the capacitors installed in the wind power plant. The reactive power consumed by the test network follows the curve of reactive power supplied by the source. A transient component of reactive power with low magnitude is also observed at the time of simultaneous outage of both wind and solar PV generators.
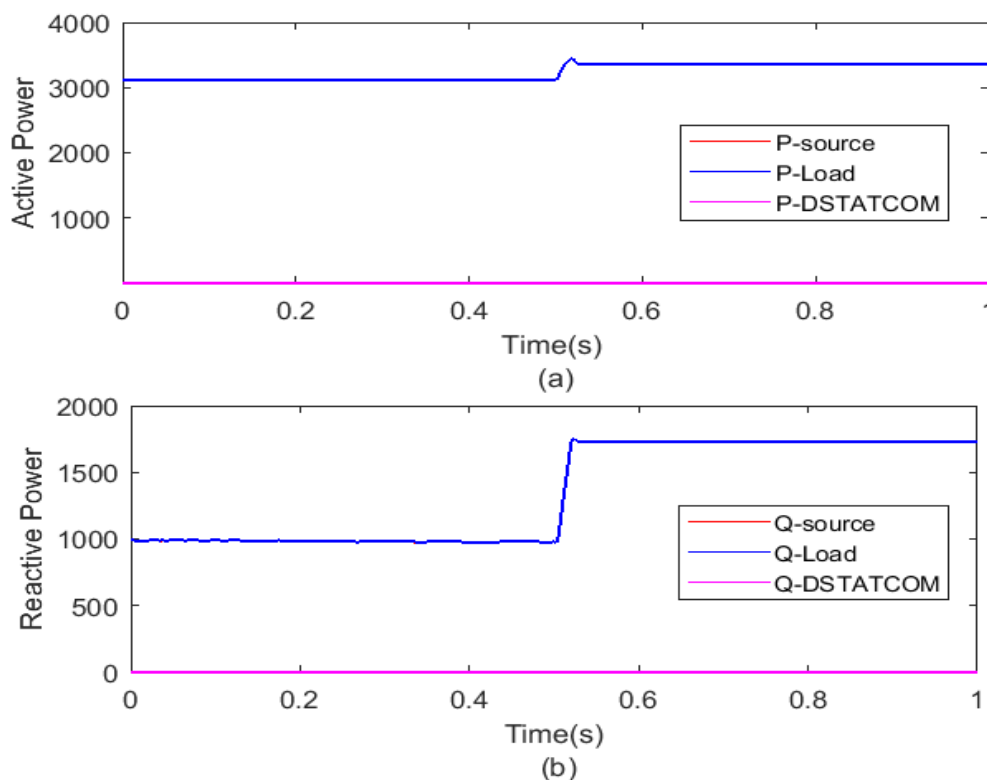


**Figure 17.** Power flow during the event of outage of wind generator without BESS (a) active power flow (b) reactive power flow.

### 3.4.2. Presence of BESS

The simultaneous outage of wind and solar PV generators integrated on bus B5 of test system is performed at 0.5 s in the presence of BESS. Voltage signal is recorded at PCC and depicted in Figure 18. It is observed that due to the event of simultaneous outage of both wind and solar PV generators in the presence of BESS the decreases by an amount of 7 V. Hence, an improvement of 3 V (50%) has been observed by the use of the BESS. The magnitude of transient voltage with sharp dip at the time of simultaneous outage of both wind and solar PV generators has been reduced significantly by the use of BESS.
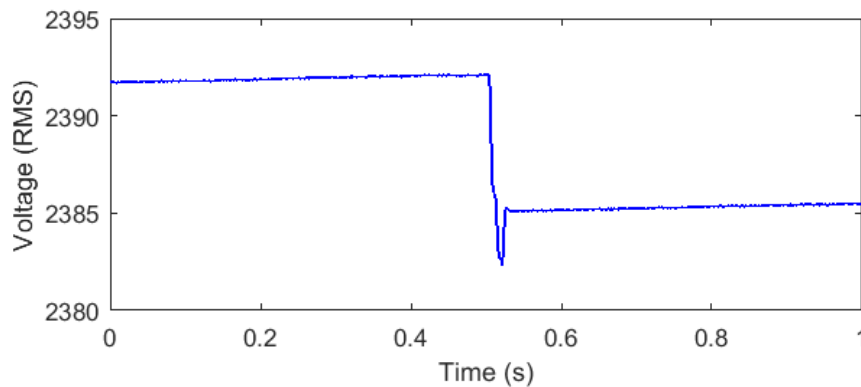


**Figure 18.** Voltage at PCC during the event of simultaneous outage of both wind and solar PV generators with BESS.
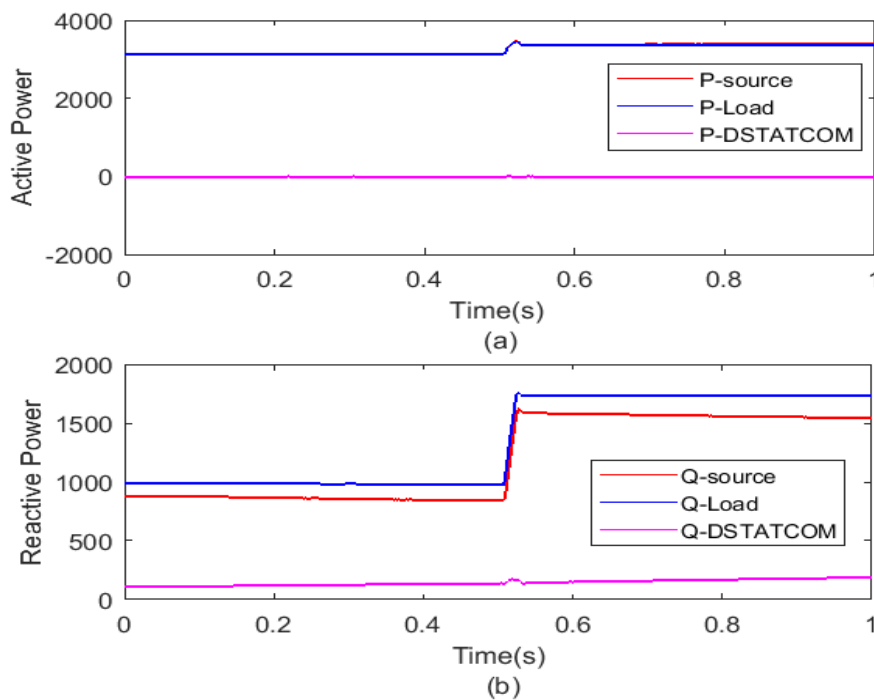


**Figure 19.** Power flow during the event of outage of both wind and solar PV generators with BESS (a) active power flow (b) reactive power flow.

The simultaneous outage of wind and solar PV generators integrated on bus B5 of test system is performed at 0.5 s in the presence of BESS. Active power supplied by the source, consumed by the load and supplied by the BESS supported by DSTATCOM is shown in Figure 19(a). Reactive power supplied by the source, consumed by the load and supplied by the BESS supported by DSTATCOM during the event of simultaneous outage of wind and solar PV generators in the presence of BESS is shown in Figure 19(b).

This can be observed from the Figure 19(a) that power supplied by the BESS is very low before and after the simultaneous outage of wind and solar PV generators. However, significant exchange of power takes place with the BESS at the time of simultaneous outage of wind and solar PV generators which helps to reduce the transient power magnitude. Hence, curve of active power consumed by load superimposes over the active power supplied by the source. Further, the active power supplied by the source increases after the event of simultaneous outage of wind and solar PV generators due to reduction in the local generation available in the test network. It is also observed by the Figure 19(b) that BESS supported by DSTATCOM continuously supplies reactive power before and after the event of outage of wind generator in the presence of BESS. Transient component of reactive power observed at the time of simultaneous outage of wind and solar PV generators has been reduced significantly by the use of BESS supported by DSTATCOM.

## 4. Performance comparison in terms of THD

Performance of proposed BESS controlled by the DSTATCOM has been tested in terms of percentage reduction in the total harmonic distortions (THD) associated with the voltage and current signals. The percentage improvement (PI) in the THD is calculated using the following relation.

$$PI = \frac{THDD - THDWD}{THDD} \times 100\%$$

where THDD is the THD in the absence of BESS controlled by DSTATCOM and THDWD is the THD in the presence of BESS controlled by DSTATCOM.

The total harmonic distortions of voltage waveforms in the presence of BESS and absence of BESS are tabulated in Table 3. This is observed that in all the events, THD of voltage waveform decreases by the use of BESS controlled by DSTATCOM. Improvement in the values of THD associated with voltage waveform during the events of switching ON the R load, switching OFF the R load, outage of wind generator and simultaneous outage of both wind and solar PV generator has been observed to be 67.95%, 50.06%, 69.63% and 68.73% respectively by the use of BESS. This indicates that the BESS reduces the transient components associated with the voltage waveform.

**Table 3.** Total harmonic distortion in voltage.

| Event | THD (%) | | Percentage improvement in THD |
|---|---|---|---|
| | *Without BESS* | *With BESS* | |
| Switching ON the R load | 1.81 | 0.58 | 67.95 |
| Switching OFF the R load | 2.27 | 1.12 | 50.06 |
| Outage of wind generator | 4.71 | 1.43 | 69.63 |
| Simultaneous outage of both wind and solar PV generator | 4.19 | 1.31 | 68.73 |

The total harmonic distortions of current waveforms in the presence of BESS and absence of BESS are tabulated in Table 4. This is observed that in all the events, THD of current waveform decreases by the use of BESS controlled by DSTATCOM. Improvement in the values of THD associated with current waveform during the events of switching ON the R load, switching OFF the R load, outage of wind generator and simultaneous outage of both wind and solar PV generator has been observed to be 51.61%, 52.39%, 57.68% and 63.06% respectively by the use of BESS. This indicates that the BESS reduces the transient components associated with the current waveform.

**Table 4.** Total harmonic distortion in current.

| Event | THD (%) | | Percentage improvement in THD |
|---|---|---|---|
| | *Without BESS* | *With BESS* | |
| Switching ON the R load | 2.17 | 1.05 | 51.61 |
| Switching OFF the R load | 3.97 | 1.89 | 52.39 |
| Outage of wind generator | 8.91 | 3.77 | 57.68 |
| Simultaneous outage of both wind and solar PV generator | 6.01 | 2.22 | 63.06 |

## 5.  Conclusions

This paper presents a technique aimed on optimized use of battery energy storage system to mitigate grid disturbances in the hybrid power system in the presence of both wind energy and solar PV energy. Active power and reactive power exchange between BESS and utility network is achieved with the help of DSTATCOM incorporated with BESS in parallel with the dc link capacitor. Control of the DSTATCOM is achieved using SRFT. Disturbances associated with operational events such as switching ON and OFF the resistive load, outage of wind generator, simultaneous outage of both wind and solar PV generators have been successfully mitigated using proposed optimistic approach. Performance of the proposed approach is evaluated in terms of improvement in voltage profile, reduction in transients of active and reactive powers by the use of BESS. Performance of BESS supported DSTATCOM is also evaluated in terms of values of THD associated with voltage and current waveforms with and without battery storage system controlled by DSTATCOM in the network. It is concluded that grid disturbances in the utility network in the hybrid power system can effectively be mitigated by the optimistic use of BESS controlled by DSTATCOM. Improvement in THD of voltage is achieved by 69% whereas current THD has been improved by 63% using the BESS. Improvement in voltage profile is achieved up to 40%. Power exchange between BESS and PCC is achieved up to 31% of rated load has been achieved by the used of BESS.

**Conflict of interest**

The authors declare no conflict of interests.

**References**

1.  Stroe DI, Zaharof A, Iov F (2018) Power and energy management with battery storage for a hybrid residential PV-wind system——a case study for Denmark. *Energ Procedia* 155: 464–477.

2. Murray P, Orehounig K, Grosspietsch D, et al. (2018) A comparison of storage systems in neighbourhood decentralized energy system applications from 2015 to 2050. *Appl energ* 231: 1285–1306.

3. Nge CL, Ranaweera IU, Midtgård OM, et al. (2019) A real-time energy management system for smart grid integrated photovoltaic generation with battery storage. *Renew energ* 130: 774–785.

4. Rohit AK, Devi KP, Rangnekar S (2017) An overview of energy storage and its importance in Indian renewable energy sector: part I—technologies and comparison. *J Energ Storage* 13: 10–23.

5. Das CK, Bass O, Kothapalli G, et al. (2018) Overview of energy storage systems in distribution networks: placement, sizing, operation, and power quality. *Renew Sust Energ Rev* 91: 1205–1230.

6. Hannan MA, Lipu MSH, Ker PJ, et al. (2019) Power electronics contribution to renewable energy conversion addressing emission reduction: applications, issues, and recommendations. *Appl Energ* 251: 113404.

7. Zhang G, Wu B, Maleki A, et al. (2018) Simulated annealing-chaotic search algorithm based optimization of reverse osmosis hybrid desalination system driven by wind and solar energies. *Sol Energ* 173: 964–975.

8. Zhang W, Maleki A, Rosen MA, et al. (2019) Sizing a stand-alone solar-wind-hydrogen energy system using weather forecasting and a hybrid search optimization algorithm. *Energ convers manage* 180: 609–621.

9. Zhang W, Maleki A, Rosen MA (2019) A heuristic-based approach for optimizing a small independent solar and wind hybrid power scheme incorporating load forecasting. *J Clean Prod* 241: 117920.

10. Maleki A, Hajinezhad A, Rosen MA (2016) Modeling and optimal design of an off-grid hybrid system for electricity generation using various biodiesel fuels: a case study for Davarzan, Iran. *Biofuels* 7: 699–712.

11. Maleki A (2019) Optimal operation of a grid-connected fuel cell based combined heat and power systems using particle swarm optimisation for residential sector. *Int J Amb Energ* DOI: 10.1080/01430750.2018.1562968.

12. Mahela OP, Shaik AG (2016) Power quality improvement in distribution network using DSTATCOM with battery energy storage system. *Int J Elec Power* 83: 229–240.

13. Maleki A (2018) Design and optimization of autonomous solar-wind-reverse osmosis desalination systems coupling battery and hydrogen energy storage by an improved bee algorithm. *Desalination* 435: 221–234.

14. Sharma SK, Palwalia DK, Shrivastava V (2019) Distributed generation integration optimization using fuzzy logic controller. *AIMS Energ* 7: 337–348.

15. Mahela OP, Shaik AG (2015) Power quality detection in distribution system with wind energy penetration using discrete wavelet transform. *Second International Conference on Advances in Computing and Communication Engineering*, Dehradun, India.

16. Sharma A, Ola R, Mahela OP (2016) Impact of grid disturbances on the output of grid connected wind power generation. *1st International Conference on Power Electronics, Intelligent Control and Energy Systems (ICPEICES)*, Delhi, India.

17. Mitra P, Venayagamoorthy GK (2009) An adaptive control strategy for DSTATCOM applications in an electric ship power system. *IEEE T Power Electr* 25: 95–104.

18. Labeeb M, Lathika BS (2011) Design and analysis of DSTATCOM using SRFT and ANN-fuzzy based control for power quality improvement. *IEEE Recent Advances in Intelligent Computational Systems*. Trivandrum, Kerala, India.

19. Singh B, Jayaprakash P, Kothari DP (2008) A T-connected transformer and three-leg VSC based DSTATCOM for power quality improvement. *IEEE T Power Electr* 23: 2710–2718.

20. Singh B, Jayaprakash P, Kothari DP (2008) Isolated H-bridge VSC Based 3-phase 4-wire DSTATCOM for power quality improvement. *IEEE International Conference on Sustainable Energy Technologies*. Singapore.

21. Singh B, Niwas R, Dube SK (2014) Load leveling and voltage control of permanent magnet synchronous generator-based DG set for standalone supply system. *IEEE T Ind Inform* 10: 2034–2043.